hep-ex/9809015 16 Sep 1998

Determination of the Deep Inelastic Contribution to the Generalised Gerasimov-Drell-Hearn Integral for the Proton and Neutron

The HERMES Collaboration

K. Ackerstaff[5], A. Airapetian[34], N. Akopov[34], I. Akushevich[6], M. Amarian[25,29,34], E.C. Aschenauer[6,13,25], H. Avakian[10], R. Avakian[34], A. Avetissian[34], B. Bains[15], S. Barrow[27], C. Baumgarten[22], M. Beckmann[12], S. Belostotski[28], J.E. Belz[4,30], T. Benisch[8], S. Bernreuther[8], N. Bianchi[10], S. Blanchard[24], J. Blouw[25], H. Böttcher[6], A. Borissov[6,14], J. Brack[4], S. Brauksiepe[12], B. Braun[22,8], B. Bray[3], S. Brons[6], W. Brückner[14], A. Brüll[14], E.E.W. Bruins[20], H.J. Bulten[18,25,33], R. Cadman[15], G.P. Capitani[10], P. Carter[3], P. Chumney[24], E. Cisbani[29], G.R. Court[17], P. F. Dal Piaz[9], P.P.J. Delheij[31], E. De Sanctis[10], D. De Schepper[20], E. Devitsin[21], P.K.A. de Witt Huberts[25], P. Di Nezza[10], M. Düren[8], A. Dvoredsky[3], G. Elbakian[34], J. Ely[4], J. Emerson[30,31], A. Fantoni[10], A. Fechtchenko[7], M. Ferstl[8], D. Fick[19], K. Fiedler[8], B.W. Filippone[3], H. Fischer[12], H.T. Fortune[27], B. Fox[4], S. Frabetti[9], J. Franz[12], S. Frullani[29], M.-A. Funk[5], N.D. Gagunashvili[7], P. Galumian[1], H. Gao[2,15], Y. Gärber[6], F. Garibaldi[29], G. Gavrilov[28], P. Geiger[14], V. Gharibyan[34], V. Gyurjyan[10], A. Golendoukhin[19,34], G. Graw[22], O. Grebeniouk[28], P.W. Green[1,31], L.G. Greeniaus[1,31], C. Grosshauser[8], M.G. Guidal[25], A. Gute[8], V. Gyurjyan[10], J.P. Haas[24], W. Haeberli[18], J.-O. Hansen[2], D. Hasch[6], O. Häusser[†,30,31], F.H. Heinsius[12], R. Henderson[31], T. Henkes[25], M. Henoch[8], R. Hertenberger[22], Y. Holler[5], R.J. Holt[15], W. Hoprich[14], H. Ihssen[5,25], M. Iodice[29], A. Izotov[28], H.E. Jackson[2], A. Jgoun[28], C. Jones[2], R. Kaiser[30,31], E. Kinney[4], M. Kirsch[8], A. Kisselev[28], P. Kitching[1], H. Kobayashi[32], N. Koch[19], K. Königsmann[12], M. Kolstein[25], H. Kolster[22], V. Korotkov[6], W. Korsch[3,34], V. Kozlov[21], L.H. Kramer[20,33], B. Krause[6], V.G. Krivokhijine[7], M. Kückes[31], F. Kümmell[12], G. Kyle[24], W. Lachnit[8], W. Lorenzon[23,27], A. Lung[3], N.C.R. Makins[2,15], S.I. Manaenkov[28], F.K. Martens[1], J.W. Martin[20], F. Masoli[9], A. Mateos[20], M. McAndrew[17], K. McIlhany[3], R.D. McKeown[3], F. Meissner[6], F. Menden[31], D. Mercer[4], A. Metz[22], N. Meyners[5] O. Mikloukho[28], C.A. Miller[1,31], M.A. Miller[15], R. Milner[20], V. Mitsyn[7], A. Most[15,27], R. Mozzetti[10], V. Muccifora[10], A. Nagaitsev[7], Y. Naryshkin[28], A.M. Nathan[15], F. Neunreither[8], M. Niczyporuk[20], W.-D. Nowak[6], M. Nupieri[10], P. Oelwein[14], H. Ogami[32], T.G. O'Neill[2], R. Openshaw[31], J. Ouyang[31], B. Owen[15], V. Papavassiliou[24], S.F. Pate[20,24], M. Pitt[3], H.R. Poolman[25], S. Potashov[21], D.H. Potterveld[2], G. Rakness[4], A. Reali[9], R. Redwine[20], A.R. Reolon[10], R. Ristinen[4], K. Rith[8], H. Roloff[6], G. Röper[5], P. Rossi[10], S. Rudnitsky[27], M. Ruh[12], D. Ryckbosch[13], Y. Sakemi[32], I. Savin[7], C. Scarlett[23], F. Schmidt[8], H. Schmitt[12], G. Schnell[24], K.P. Schüler[5], A. Schwind[6], J. Seibert[12], T.-A. Shibata[32], T. Shin[20], V. Shutov[7], M.C. Simani[9] A. Simon[12,24], K. Sinram[5], P. Slavich[9,10], W.R. Smythe[4], J. Sowinski[14], M. Spengos[5,27], E. Steffens[8], J. Stenger[8], J. Stewart[17], F. Stock[14,8], U. Stoesslein[6], M. Sutter[20], H. Tallini[17], S. Taroian[34], A. Terkulov[21], D.M. Thiessen[31], E. Thomas[10], B. Tipton[20], A. Trudel[31], M. Tytgat[13], G.M. Urciuoli[29], J.J. van Hunen[25], R. van de Vyver[13], J.F.J. van den Brand[25,33], G. van der Steenhoven[25], M.C. Vetterli[30,31], M. Vincter[31], J. Visser[25], E. Volk[14], W. Wander[8], T.P. Welch[26], S.E. Williamson[15], T. Wise[18], K. Woller[5], S. Yoneyama[32], K. Zapfe-Düren[5], H. Zohrabian[34], R. Zurmühle[27]

[1] *Department of Physics, University of Alberta, Edmonton, Alberta T6G 2J1, Canada*
[2] *Physics Division, Argonne National Laboratory, Argonne, Illinois 60439, USA*
[3] *W.K. Kellogg Radiation Lab, California Institute of Technology, Pasadena, California, 91125, USA*
[4] *Nuclear Physics Laboratory, University of Colorado, Boulder, Colorado 80309-0446, USA*
[5] *DESY, Deutsches Elektronen Synchrotron, 22603 Hamburg, Germany*
[6] *DESY Zeuthen, 15738 Zeuthen, Germany*
[7] *Joint Institute for Nuclear Research, 141980 Dubna, Russia*
[8] *Physikalisches Institut, Universität Erlangen-Nürnberg, 91058 Erlangen, Germany*
[9] *Istituto Nazionale di Fisica Nucleare and Dipartimento di Fisica, Università di Ferrara, 44100 Ferrara, Italy*
[10] *Istituto Nazionale di Fisica Nucleare, Laboratori Nazionali di Frascati, 00044 Frascati, Italy*
[11] *Department of Physics, Florida International University, Miami, Florida 33199, USA*
[12] *Fakultät für Physik, Universität Freiburg, 79104 Freiburg, Germany*
[13] *Department of Subatomic and Radiation Physics, University of Gent, 9000 Gent, Belgium*
[14] *Max-Planck-Institut für Kernphysik, 69029 Heidelberg, Germany*
[15] *Department of Physics, University of Illinois, Urbana, Illinois 61801, USA*
[16] *Department of Physics and Astronomy, University of Kentucky, Lexington, Kentucky 40506,USA*
[17] *Physics Department, University of Liverpool, Liverpool L693BX, United Kingdom*
[18] *Department of Physics, University of Wisconsin-Madison, Madison, Wisconsin 53706, USA*
[19] *Physikalisches Institut, Philipps-Universität Marburg, 35037 Marburg, Germany*
[20] *Laboratory for Nuclear Science, Massachusetts Institute of Technology, Cambridge, Massachusetts 02139, USA*
[21] *Lebedev Physical Institut, 117924 Moscow, Russia*
[22] *Sektion Physik der Universität München, 85748 Garching, Germany*
[23] *Randall Laboratory of Physics, University of Michigan, Ann Arbor, Michigan 48109-1120, USA*

[24] *Department of Physics, New Mexico State University, Las Cruces, New Mexico 88003, USA*
[25] *Nationaal Instituut voor Kernfysica en Hoge-Energiefysica (NIKHEF), 1009 DB Amsterdam, The Netherlands*
[26] *University of Oregon, Eugene, Oregon 97403 USA*
[27] *University of Pennsylvania, Philadelphia Pennsylvania 19104, USA*
[28] *Petersburg Nuclear Physics Institute, St. Petersburg, 188350 Russia*
[29] *Istituto Nazionale di Fisica Nucleare, Sezione Sanità, and Istituto Superiore di Sanità, Physics Laboratory, 00161 Roma, Italy*
[30] *Department of Physics, Simon Fraser University, Burnaby, British Columbia V5A 1S6 Canada*
[31] *TRIUMF, Vancouver, British Columbia V6T 2A3, Canada*
[32] *Tokyo Institute of Technology, Tokyo 152, Japan*
[33] *Department of Physics and Astronomy, Vrije Universiteit, 1081 HV Amsterdam, The Netherlands*
[34] *Yerevan Physics Institute, 375036, Yerevan, Armenia*

The virtual photon absorption cross section differences $[\sigma_{1/2} - \sigma_{3/2}]$ for the proton and neutron have been determined from measurements of polarised cross section asymmetries in deep inelastic scattering of 27.5 GeV longitudinally polarised positrons from polarised ^{1}H and ^{3}He internal gas targets. The data were collected in the region above the nucleon resonances in the kinematic range $\nu < 23.5$ GeV and 0.8 GeV$^2 < Q^2 < 12$ GeV^2. For the proton the contribution to the generalised Gerasimov-Drell-Hearn integral was found to be substantial and must be included for an accurate determination of the full integral. Furthermore the data are consistent with a QCD next-to-leading order fit based on previous deep inelastic scattering data. Therefore higher twist effects do not appear significant.
PACS numbers : 13.60.Hb; 13.88.+e; 25.20.Dc; 25.30.Fj
Keywords : Deep Inelastic Scattering, Sum Rules, Asymmetries, Photo-absorption

The GDH sum rule, derived in the sixties by Gerasimov [1] and independently by Drell and Hearn [2], relates the anomalous contribution κ to the magnetic moment of the nucleon ($\kappa_{\rm p}$=1.79, $\kappa_{\rm n}$=−1.91) with the total absorption cross sections for circularly polarised real photons on polarised nucleons. It is written as:

$$\int_0^\infty \Big[\sigma_{1/2}(\nu) - \sigma_{3/2}(\nu)\Big]\frac{d\nu}{\nu} = -\frac{2\pi^2\alpha}{M^2}\kappa^2, \qquad (1)$$

where $\sigma_{1/2}$ and $\sigma_{3/2}$ are the photo-absorption cross sections for total helicities 1/2 and 3/2, ν is the photon energy, and M is the nucleon mass. The sum rule arises from the combination of a general dispersion relation for forward Compton scattering [3] and the low-energy theorem of Low [4], with the additional assumption that the spin-flip part of the Compton scattering amplitude goes to zero at infinite energy without any poles. The theoretical predictions for the integral are −204 μb and −233 μb for the proton and neutron, respectively. Experimentally this sum rule has never been tested directly because of the lack of suitable polarised real photon beams.

The integral defined in Eq. 1 can be generalised to the absorption of virtual photons with energy ν and squared four-momentum $-Q^2$:

$$I(Q^2) \equiv \int_{Q^2/2M}^\infty \Big[\sigma_{1/2}(\nu,Q^2) - \sigma_{3/2}(\nu,Q^2)\Big]\frac{d\nu}{\nu}$$
$$= \frac{8\pi^2\alpha}{M}\int_0^1 \frac{g_1(x,Q^2) - \gamma^2 g_2(x,Q^2)}{K}\frac{dx}{x}. \qquad (2)$$

Here g_1 and g_2 are the polarised structure functions of the nucleon, x is the Bjorken variable and $K = \nu\sqrt{1+\gamma^2}$ is the flux factor of the virtual photons [5], with $\gamma^2 = Q^2/\nu^2$. For Q^2=0 the left side of Eq. 2 is trivially equal to the left side of Eq. 1. The Q^2 dependence of this integral connects the static ground state properties of the nucleon with its helicity structure as measured in inelastic scattering in the resonance and deep inelastic regions.

Interest in the generalised GDH integral arose in 1989 when it was related [6] to $\Gamma_1 = \int_0^1 g_1(x)dx$, which had been measured [7,8] to be significantly smaller than expected [9]. In fact, for $\gamma \ll 1$, the right side of Eq. 2 reduces to $I_1(Q^2) \equiv 16\pi^2\alpha\Gamma_1/Q^2$. For both neutron and proton a strong variation of $I(Q^2)$ is required in order to connect Γ_1 to the GDH prediction for real photons; in the case of the proton Γ_1 is positive and then $I(Q^2)$ must change sign at low Q^2. Several possible explanations of this behaviour have been proposed [10-16] – for example the contributions of the resonances, of g_2 and of higher twist effects to the Q^2-evolution of the integral were taken into consideration.

This letter presents results for the cross section differences $[\sigma_{1/2} - \sigma_{3/2}]$ extracted from measurements of the longitudinal positron-nucleon cross section asymmetries $A_{||}$ for the neutron and the proton in the deep inelastic scattering (DIS) region. The data were collected during the 1995 and 1997 years of operation of the HERMES experiment. The 1995 ^{3}He data for the neutron have previously been used for the extraction of the polarised structure function $g_1^{\rm n}(x)$ [17]; the 1997 ^{1}H data have been used for the determination of $g_1^{\rm p}(x)$ [18].

The experiment was performed with a 27.5 GeV beam of longitudinally polarised positrons incident on longitudinally polarised ^{1}H and ^{3}He gas targets internal to

the HERA storage ring at DESY. The positron beam in the HERA ring is transversely polarised by emission of synchrotron radiation [19]. Longitudinal polarisation is obtained by using spin rotators located upstream and downstream of the HERMES experiment [20]. The average beam polarisation for the analysed data was 0.55 with a relative systematic uncertainty of 3.4% (3.9%) for the proton (neutron).

The ^{1}H target atoms are produced by an atomic beam source (ABS) based on Stern-Gerlach separation of atomic hydrogen spin states [21]. The ^{3}He target atoms are polarised by spin exchange collisions with optically-pumped ^{3}He atoms in the 2^3S meta-stable state [22]. The beam of polarised atoms enters a 400 mm long open-ended thin-walled storage cell located inside the storage ring, providing an areal target density of approximately 7×10^{13} ^{1}H-atoms/cm^2 or 3.3×10^{14} ^{3}He-atoms/cm^2. The average values of the target polarisation during the experiment were 0.88 ± 0.04 for ^{1}H [18] and 0.46 ± 0.02 for ^{3}He [17].

The magnetic spectrometer is fully described in Ref. [23]. It is constructed as two identical halves mounted above and below the positron ring plane. The angular acceptance of the spectrometer extends over the range 40 mrad $< \theta <$ 220 mrad. For positrons the average angular resolution is better than 1 mrad and the average momentum resolution is better than 2% aside from bremsstrahlung tails. Positron identification is accomplished with a lead glass calorimeter, a preshower counter, a transition radiation detector and a gas threshold Čerenkov counter. For the analysed data sets the hadron contamination was less than 1% at an average positron identification efficiency of 99%.

The cross section difference $[\sigma_{1/2} - \sigma_{3/2}]$ can be expressed in terms of the virtual photo-absorption asymmetry A_1 and the unpolarised structure function F_1:

$$\sigma_{1/2} - \sigma_{3/2} = \frac{8\pi^2\alpha}{M}\,\frac{A_1 F_1}{K}. \qquad (3)$$

The structure function $F_1 = F_2(1+\gamma^2)/(2x(1+R))$ was calculated from published parameterisations of the unpolarised structure function F_2 [24] and of $R = \sigma_L/\sigma_T$ [25], the ratio of the absorption cross sections for longitudinally and transversely polarised virtual photons. The asymmetry A_1 was extracted from the measured longitudinal asymmetry $A_{\|}$ by means of the formula $A_1 = A_{\|}/D - \eta A_2$, where $D = y(2-y)(1+\gamma^2 y/2)/[y^2(1+\gamma^2)(1-2m_e^2/Q^2)+2(1-y-\gamma^2 y^2/4)(1+R)]$ is the virtual photon depolarisation factor (m_e is the electron mass), $\eta = \gamma(1-y-\gamma^2 y^2/4)/(1-y/2)(1+\gamma^2 y/2)$ and $y = \nu/E$, where E is the beam energy. The asymmetry A_2 is bounded by the positivity limit $A_2 \leq \sqrt{R}$ and has been measured to be small [26-28]; moreover, the factor η is less than 0.5 in the kinematic range covered by this analysis. The contribution of A_2 for the proton was evaluated with a parameterization $A_2^p = 0.5x/\sqrt{Q^2}$ based on existing data [27,28], while the contribution of A_2 for the neutron was neglected and the uncertainty [26] was included in the systematic error.

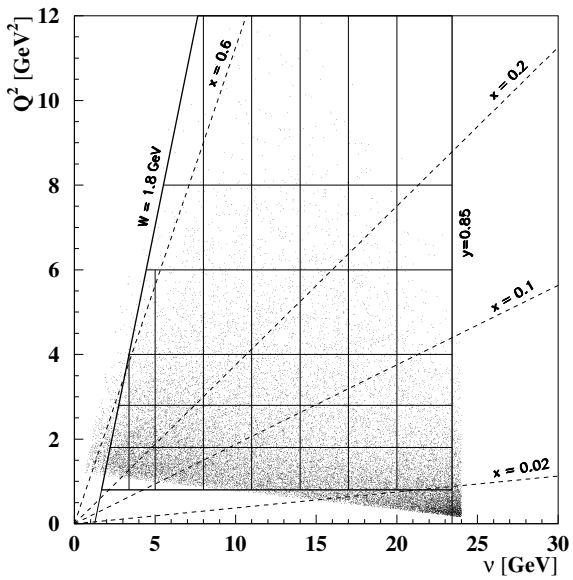

FIG. 1. Kinematic plane covered by the HERMES experiment showing the boundaries and the binning in Q^2 and ν used for the evaluation of the GDH integral for the proton data above the resonance region. The points shown are a sample of the whole set of collected data.

After applying data quality criteria, 1.8 (2.7) million events for the proton (helium) target were available in the kinematic range $0.8\ \mathrm{GeV}^2 < Q^2 < 12$ (10) GeV^2, $\nu <$ 23.5 GeV and $W > W_0 = 1.8$ (2) GeV, where W is the energy of the hadronic final state. The kinematic plane covered by this experiment is shown in Fig. 1. Above the minimum angle of 40 mrad the events are continously distributed allowing – without interpolation – the integration over ν for several bins in Q^2.

The x-range covered in the different Q^2-bins varied from 0.03–0.36 for the lowest Q^2-bin to 0.2–0.8 for the highest one. The kinematic range for the proton was slightly increased compared to that of the neutron due to the intrinsically higher figure of merit of the ^{1}H target.

The value of $A_{\|}/D$ has been extracted in each bin by using

$$\frac{A_{\|}}{D} = \frac{1}{D}\,\frac{N^- L^+ - N^+ L^-}{N^- L_P^+ + N^+ L_P^-}, \qquad (4)$$

where N is the number of detected scattered positrons corrected for e^+e^- background from charge symmetric processes. Here L is the integrated luminosity corrected for dead time; L_P is the integrated luminosity corrected for dead time and weighted by the product of beam and target polarisations. The superscript + (−) refers to the situation where the target spin axis was oriented parallel

(anti-parallel) to that of the positron beam. Radiative corrections are typically 2% of the observed asymmetry for the proton and 20% for the neutron. They were calculated using the prescription given in Ref. [29]. The neutron asymmetry A_1^n was obtained from the ^{3}He asymmetry by correcting for nuclear effects, assuming a relative polarisation of 0.86 ± 0.02 for the neutron and -0.028 ± 0.004 for each of the two protons in the ^{3}He nucleus [30], and using a fit of data for A_1^p [31].

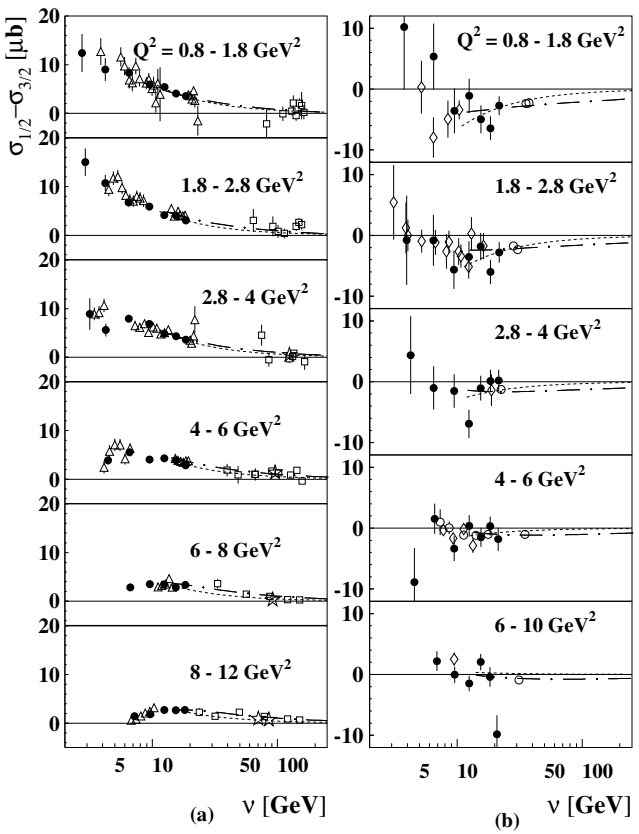

FIG. 2. Cross section differences as a function of ν measured in different bins of Q^2 for the proton (a) and the neutron (b). Filled circles are data from this experiment. Open symbols are values derived from other experiments: stars [7], triangles [27], squares [28], diamonds [32], and circles [33]. Only statistical uncertainties are given. The dashed curves are ν^{-1} Regge fits to the HERMES data with $W > 4.5$ GeV; the dash-dotted curves show the next-to-leading order QCD parameterization [34].

The cross section differences $[\sigma_{1/2} - \sigma_{3/2}]$ calculated from the extracted values of A_1^p and A_1^n by means of Eq. 3 are presented in Fig. 2. They are compared to the values of $[\sigma_{1/2} - \sigma_{3/2}]$ determined from the published data from other experiments for A_1^p using polarised proton targets [7,27,28] and for A_1^n using polarised helium-3 targets [32,33]. There is good agreement between different experiments in the overlapping kinematic regions. Note that the data of Refs. [27,32,33] were obtained at fixed scattering angles and are therefore restricted to kinematic regions that are highly correlated in ν and Q^2. An evaluation of the integrals $I(Q^2)$ with these data would thus require interpolations.

All HERMES values for the proton are clearly positive, ranging between about 1 μb and about 16 μb. Most of the data for the neutron at $\nu \geq 8$ GeV are negative, ranging between about -10 μb and 0 μb. In each Q^2-bin the present data for the cross section difference $[\sigma_{1/2} - \sigma_{3/2}]$ has been multiplied by $1/\nu$ and integrated over the range $\nu_0 < \nu < 23.5$ GeV, with $\nu_0 = (W_0^2 - M^2 + Q^2)/2M$. In the integration the ν dependence of the integrand $F_1/(K\nu)$ within the individual ν-bins was fully accounted for. The data listed in Tab. 1 and shown in Fig. 3 represent the DIS component for the HERMES kinematic range $I^{\rm DIS}_{\rm HERMES}(Q^2)$ of $I(Q^2)$. For the proton this contribution decreases from about 21 μb at $Q^2 = 1.3$ GeV^2 to about 3 μb at $Q^2 = 9.3$ GeV^2. The contribution for the neutron is smaller in absolute value and between -5 μb and +8 μb.

Table 1: Results on $I^{\rm DIS}_{\rm HERMES}(Q^2)$ for the proton and neutron.

Proton	
Q^2 [GeV^2]	$I^{\rm DIS}_{\rm HERMES}(Q^2) \pm$ stat. $\pm$ syst. [μb]
1.28	20.9 ± 3.0 ± 2.6
2.23	16.6 ± 1.2 ± 1.8
3.31	11.8 ± 0.7 ± 1.1
4.79	7.3 ± 0.4 ± 0.6
6.81	4.7 ± 0.3 ± 0.4
9.25	2.9 ± 0.4 ± 0.2
Neutron	
Q^2 [GeV^2]	$I^{\rm DIS}_{\rm HERMES}(Q^2) \pm$ stat. $\pm$ syst. [μb]
1.28	7.5 ± 9.2 ± 2.6
2.23	-5.2 ± 4.5 ± 1.3
3.31	-1.3 ± 3.0 ± 1.1
4.79	-2.1 ± 1.6 ± 0.6
7.25	-0.9 ± 0.9 ± 0.4

The sizes of the systematic uncertainties are indicated by the bands at the bottom of Figs. 3a and 3b. The main contributions are those from the beam and target polarisations. Other sources are uncertainties in A_2, in radiative and smearing corrections, and in the knowledge of the unpolarised structure functions F_2 and R. For the lowest Q^2 bin the uncertainty due to the knowledge of A_2 is dominant. In addition, for the neutron there is a contribution from the nuclear corrections.

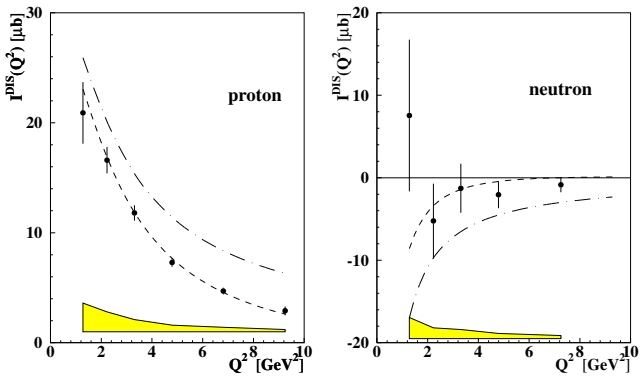

(a) (b)

FIG. 3. The generalised GDH integral as a function of Q^2 in the deep inelastic region. The points are $I^{\rm DIS}_{\rm HERMES}(Q^2)$ as measured for HERMES data in the range $\nu_0 \leq \nu \leq 23.5$ GeV for the proton (a) and for the neutron (b). The error bars show the statistical uncertainties and the bands represent the systematic uncertainties. See text for the explanation of the curves.

The data are compared with estimates of the integrals that do not include contributions from nucleon resonances or possible higher twist effects. These estimates were derived using a parameterization [34] for the asymmetry A_1 given by a next-to-leading order (NLO) QCD analysis. Note that a number of the low Q^2, low ν data points shown in Fig. 2 from Ref. [27] are not used in this parameterisation. The dashed curves in Fig. 3 show the integrals for this parameterisation over the x range measured at HERMES for proton and neutron. They are in good agreement with all data, indicating that higher twist effects do not contribute significantly in the deep inelastic region, even at the lowest measured Q^2. The dash-dotted curves show the integrals of the NLO parameterisation from ν_0 to infinity, thus including in addition the low x (high ν) contribution, which for the proton is about 4μb.

An alternative approach was also used to account for the high ν region. It is well known that the applicability of the simple Regge picture is uncertain and that the asymptotic behaviour of $[\sigma_{1/2}(\nu) - \sigma_{3/2}(\nu)]$ at higher energy or $g_1(x)$ at low x requires a more refined treatment [35,36]. However, if a Regge behaviour is assumed here for the sake of comparison, the main high ν contribution comes from the $a_1(1260)$ Regge trajectory such that $[\sigma_{1/2} - \sigma_{3/2}] \propto \nu^{\alpha-1}$, where α is the intercept of this trajectory. The present data with $W \geq 4.5$ GeV have been fitted with such a parameterisation using $\alpha = 0$ [37]. Fits are shown as dashed curves in Fig. 2; they are in fair agreement with data. The contribution of the high ν Regge extrapolation to the integral is about 3 μb for the proton data, as well as for the neutron data with $Q^2 < 4$ GeV^2.

Little experimental information is available about the size of the resonance contribution to $I(Q^2)$. Up to now the resonance part ($W < 2$ GeV) of Γ_1 has been determined only for two Q^2 values (0.5 GeV^2 and 1.2 GeV^2) [27,38]. This contribution has been compared to the part of Γ_1 at larger W and at the same fixed Q^2, obtained by interpolating to the appropriate Q^2 the data taken at fixed scattering angles of 4.5 and 7 degrees and at the two beam energies 9.7 GeV and 16.2 GeV. For example at $Q^2 = 1.2$ GeV^2, the resonance contribution was found to be about 37% of the whole integral Γ_1 for the proton, including a negative contribution from the first resonance [27,39].

A measurement of A_1 and A_2 is planned at TJNAF [40] for a determination of the contribution of the resonance region to the generalised GDH integral $I(Q^2)$ for $Q^2 < 3$ GeV^2. This together with the present results in the deep inelastic scattering regime and a more refined estimate of the high energy extrapolation will provide the Q^2 evolution of the entire integral. In addition, several experiments are planned at different facilities to measure the spin-dependent photo-production cross sections to test the GDH sum rule for real photons [41].

In conclusion, the polarised cross section differences $[\sigma_{1/2} - \sigma_{3/2}]$ have been determined for the proton and neutron in the kinematic range 0.8 GeV^2 $< Q^2 <$ 12 GeV^2, $W > 1.8$ GeV, $\nu < 23.5$ GeV, and the corresponding DIS parts of the generalised GDH integrals $I(Q^2)$ have been evaluated. For Q^2 above 1 GeV^2 the results are at least of the same order of magnitude as expectations for the resonance part of $I(Q^2)$. Therefore the rapid excursion of $I(Q^2)$ towards the predicted negative values at Q^2=0 must occur below a Q^2 of about 1 GeV^2. Furthermore the data are consistent with a QCD next-to-leading order fit based on previous deep inelastic scattering data, indicating that higher twist effects are not significant even at the lowest measured Q^2.

We gratefully acknowledge the DESY management for its support and the staffs at DESY and the collaborating institutions for their significant effort. This work was supported by the Fund for Scientific Research-Flanders (FWO) of Belgium; the Natural Sciences and Engineering Research Council of Canada; the INTAS, HCM and TMR contributions from the European Community; the German Bundesministerium für Bildung, Wissenschaft, Forschung und Technologie (BMBF), the Deutscher Akademischer Austauschdienst (DAAD); the Italian Istituto Nazionale di Fisica Nucleare (INFN); Monbusho, JSPS, and Toray Science Foundation of Japan; the Dutch Stichting voor Fundamenteel Onderzoek der Materie (FOM); the UK Particle Physics and Astronomy Research Council; and the US Department of Energy and National Science Foundation.

† Deceased.

[1] S.B. Gerasimov, Sov. J. Nucl. Phys. **2** (1966) 430.
[2] S.D. Drell and A.C. Hearn, Phys. Rev. Lett. **16** (1966) 908.
[3] M. Gell-Mann *et al.*, Phys. Rev. **95** (1954) 1612.
[4] F.E. Low, Phys. Rev. **96** (1954) 1428.
[5] F.J. Gilman, Phys. Rev. **167** (1968) 1365.
[6] M. Anselmino, B.L. Ioffe and E. Leader, Sov. J. Nucl. Phys. **49** (1989) 136.
[7] EMC Collaboration, J. Ashman *et al.*, Nucl. Phys. **B 328** (1989) 1.
[8] E130 Collaboration, G. Baum *et al.*, Phys. Rev. Lett. **51** (1983) 1135.
[9] J. Ellis and R.L. Jaffe, Phys. Rev. **D 9** (1974) 1444; Phys. Rev. **D 10** (1974) 1669.
[10] V.D. Burkert and B.L. Ioffe, Phys. Lett. **B 296** (1992) 223.
[11] V.D. Burkert and Z. Li, Phys. Rev. **D 47** (1993) 46.
[12] Z. Li, Phys. Rev. **D 47** (1993) 1854.
[13] J. Soffer and O. Teryaev, Phys. Rev. Lett. **70** (1993) 3373.
[14] X. Ji, Phys. Lett. **B 309** (1993) 187.
[15] Z. Li *et al.*, Phys. Rev. **D 46** (1992) 70.
[16] Z. Li and Z. Li, Phys. Rev. **D 50** (1994) 3119.
[17] HERMES Collaboration, K. Ackerstaff *et al.*, Phys. Lett. **B 404** (1997) 383.
[18] HERMES Collaboration, A. Airapetian *et al.*, DESY 98-072 (1998), hep-ex 9807015 (1998), Phys. Lett. **B** (in press).
[19] A.A. Sokolov and I.M. Ternov, Sov. Phys. Doklady **8** (1964) 1203.
[20] D.P. Barber *et al.*, Phys. Lett. **B 343** (1997) 436.
[21] F. Stock *et al.*, Nucl. Instr. and Meth. **343** (1994) 334.
[22] D. De Schepper *et al.*, MIT-LNS preprint 01/97, (1997).
[23] HERMES Collaboration, K. Ackerstaff *et al.*, DESY 98-057 (1998), hep-ex 9806008 (1998), Nucl. Instr. and Meth. **A** (in press).
[24] NMC Collaboration, M. Arneodo *et al.*, Phys. Lett. **B 364** (1995) 107.
[25] L.W. Whitlow *et al.*, Phys. Lett. **B 250** (1990) 193.
[26] E154 Collaboration, K. Abe *et al.*, Phys. Lett. **B 404** (1997) 377.
[27] E143 Collaboration, K. Abe *et al.*, Phys. Rev. Lett. **76** (1996) 587; K. Abe *et al.*, SLAC-PUB-7753, hep-ph 9802357 (1998).
[28] SMC Collaboration, B. Adeva *et al.*, Phys. Lett. **B 412** (1997) 414; CERN-EP 98/085 (1998).
[29] I.V. Akushevich and N.M. Shumeiko, J. Phys. **G 20** (1994) 513.
[30] J.L. Friar *et al.*, Phys. Rev. **C 42** (1990) 2310; C. Ciofi degli Atti *et al.*, Phys. Rev. **C 48** (1993) R968.
[31] E143 Collaboration, K. Abe *et al.*, Phys. Lett. **B 364** (1995) 61.
[32] E142 Collaboration, P.L. Anthony *et al.*, Phys. Rev. **D 54** (1996) 6620.
[33] E154 Collaboration, K. Abe *et al.*, Phys. Rev. Lett. **79** (1997) 26.
[34] M. Glück *et al.*, Phys. Rev. **D 53** (1996) 4775.
[35] E. Leader *et al.*, hep-ph 9807251 (1998).
[36] E154 Collaboration, K. Abe *et al.*, Phys. Lett. **B 405** (1997) 180; SMC Collaboration CERN-EP 98-086 (1998).
[37] R.L. Heimann, Nucl. Phys. **B 64** (1973) 429.
[38] E143 Collaboration, K. Abe *et al.*, Phys. Rev. Lett. **78** (1997) 815.
[39] G. Baum *et al.*, Phys. Rev. Lett. **45** (1980) 2000.
[40] V.D. Burkert *et al.*, CEBAF PR-91-23 (1991); S. Kuhn *et al.*, CEBAF PR-93-09 (1993); Z.E. Meziani *et al.*, CEBAF PR-94-10 (1994); J.P. Chen *et al.*, TJNAF PR-97-110 (1997).
[41] N. Bianchi, Proc. Workshop on Electron Nucleus Scattering, O. Benhar and A. Fabrocini Eds., Elba, July 1-5, 1996, p.363 and references therein.